



PET imaging of tumor hypoxia using ^{18}F -labeled pimonidazole

Morten Busk, Steen Jakobsen, Michael R. Horsman, Lise S. Mortensen, Ane B. Iversen, Jens Overgaard, Marianne Nordmark, Xiaosheng Ji, David Y. Lee & James R. Raleigh

To cite this article: Morten Busk, Steen Jakobsen, Michael R. Horsman, Lise S. Mortensen, Ane B. Iversen, Jens Overgaard, Marianne Nordmark, Xiaosheng Ji, David Y. Lee & James R. Raleigh (2013) PET imaging of tumor hypoxia using ^{18}F -labeled pimonidazole, Acta Oncologica, 52:7, 1300-1307, DOI: [10.3109/0284186X.2013.815797](https://doi.org/10.3109/0284186X.2013.815797)

To link to this article: <https://doi.org/10.3109/0284186X.2013.815797>



Published online: 21 Aug 2013.



Submit your article to this journal [↗](#)



Article views: 1812



View related articles [↗](#)



Citing articles: 2 View citing articles [↗](#)

ORIGINAL ARTICLE

PET imaging of tumor hypoxia using ^{18}F -labeled pimonidazole

MORTEN BUSK¹, STEEN JAKOBSEN², MICHAEL R. HORSMAN¹,
LISE S. MORTENSEN¹, ANE B. IVERSEN³, JENS OVERGAARD¹,
MARIANNE NORDSMARK¹, XIAOSHENG JI⁴, DAVID Y. LEE⁵ & JAMES R. RALEIGH⁶

¹Department of Experimental Clinical Oncology, Aarhus University Hospital (AUH), Aarhus, Denmark, ²PET Centre, AUH, Aarhus, Denmark, ³Department of Oncology, Aarhus University Hospital (AUH), Aarhus, Denmark, ⁴Hypoxprobe, Inc., Burlington, Massachusetts, USA, ⁵MacLean Hospital, Harvard Medical School, MA, USA and ⁶Department of Radiation Oncology, UNC School of Medicine, Chapel Hill, NC, USA

Abstract

Background. Tumor hypoxia contributes to loco-regional failure, and for optimal treatment planning, knowledge about tumor hypoxia in individual patients is required. Nitroimidazole-based tracers, which are retained in hypoxic cells, allow PET-based assessment of tumor hypoxia, but current tracers are characterized by slow tracer retention and clearance, resulting in low inter-tissue contrast. Pimonidazole is an immune detectable hypoxia marker widely used for detection of hypoxia in tumor samples. Pimonidazole has excellent chemical properties for hypoxia imaging, but labeling for non-invasive assay has not been attempted. Here we labeled pimonidazole with ^{18}F (^{18}F FPIMO). **Material and methods.** ^{18}F FPIMO was produced by fluorination of 1-[2-*O*-tosyl-3-(2-nitroimidazole-1-yl)-propyl]-piperidine, which resulted in two isomeric interchangeable forms (named “5” and “6”) with a radiochemical purity of 91–100%. ^{18}F FPIMO was tested by incubation of two different tumor cell lines at high and low oxygen levels. ^{18}F FPIMO was also administered to tumor-bearing mice and tracer retention in tumors, non-hypoxic reference tissues and tissues involved in drug metabolism/clearance was evaluated by various techniques. **Results and conclusions.** Retention of ^{18}F FPIMO was strongly hypoxia-driven in vitro, but isomeric form “5” was particularly promising and reached impressive anoxic-to-oxic retention ratios of 36 and 102, in FaDu_{DD} and SiHa cells, respectively, following three hours of tracer incubation. This was equal to or higher than ratios measured using the established hypoxia tracer ^{18}F FAZA. ^{18}F FPIMO also accumulated in tumors grown in mice, and reached tumor levels that were two to six-fold higher than in muscle three hours post-administration. Furthermore, the intra-tumoral distribution of ^{18}F FPIMO (autoradiography) and unlabeled pimonidazole (immunohistochemistry) was largely identical. Nonetheless, ^{18}F FPIMO proved inferior to ^{18}F FAZA, since absolute tumor signal and intra-tumoral contrast was low, thus compromising PET imaging. Low tumor signal was coupled to extensive tracer accumulation in liver and kidneys, and analysis of blood metabolites revealed that ^{18}F FPIMO was metabolized rapidly, with little parent compound remaining 15 minutes post-administration. Ongoing work focuses on the possibility of labeling pimonidazole in different positions with ^{18}F to improve tracer stability in vivo.

Due to a disorganized and poorly functioning tumor vasculature, areas with viable hypoxic cells are present in most solid tumors [1]. Hypoxic tumor cells constitute a major problem in the clinic, since the efficacy of radiotherapy is dramatically reduced at low pO_2 [1,2]. Typically, a three-fold increase in radiation dose is needed to accomplish the same cell killing in the absence of oxygen, as compared to well-oxygenated conditions [1,2]. Hypoxia also limits the efficacy of most chemotherapy, since accessibility to

hypoxic cells is reduced and hypoxic cells are typically in a non-dividing state [2]. Hypoxic intervention has shown promise and the radiosensitizer nimorazole is currently standard therapy in head and neck cancer patients eligible for radiotherapy in Denmark [3]. To optimize treatment efficacy and limit adverse effects, however, there is a need to identify patients that will benefit from specialized hypoxia-targeting treatment. Invasive analysis using oxygen electrodes or biopsy-based analysis of administered

bioreductive probes (e.g. pimonidazole) that are retained in hypoxic cells or hypoxia-regulated genes [4–7] allows assessment of tumor hypoxia. Recently, our group showed that a 15-gene hypoxia classifier were able to identify those patients that benefit from nimorazole [8,9]. However, non-invasive and easily repeatable imaging approaches are clinically more attractive, and for some treatments like image-guided dose escalation to resistant hypoxic tumor volumes [10,11], three-dimensional (3D) information on tumor hypoxia is required.

PET is a promising and clinically attractive imaging technology for the assessment of hypoxia [12–15]. Fluoromisonidazole ([¹⁸F]FMISO), an ¹⁸F-labeled nitroimidazole, was the first PET hypoxia imaging agent that was developed and tested [16]. [¹⁸F]FMISO, like other nitroimidazoles, is reduced at low oxygen levels ($\sim pO_2 < 10$ mmHg), which results in the formation of reactive intermediates that binds to macromolecules (especially protein) thus leading to tracer accumulation in poorly oxygenated yet viable tissue. Due to the limited accessibility of hypoxic cells, hypoxia-driven tumor tissue retention and clearance of unbound tracer is a very slow process. Even when PET scans are performed several hours (typically two to four hours) after tracer administration, inter-tissue and intra-tumoral contrast and absolute signal remains low, which may severely compromise the quantitative accuracy and detection limit of hypoxia PET [17,18]. Second generation hypoxia tracers such as [¹⁸F]FAZA and [¹⁸F]HX4 clear more rapidly from the circulation than [¹⁸F]FMISO due to reduced lipophilicity [19,20], and will probably replace [¹⁸F]FMISO in the future. Still, the use of these tracers only results in marginally better tumor-to-reference tissue contrast (e.g. [19,21]) and the development of novel tracers is justified.

Pimonidazole, commercialized as hypoxyprobe, is an unlabeled nitroimidazole which can be visualized hours to days after intravenous or oral administration [22] in biopsies by immunohistochemical techniques. Pimonidazole is widely used both preclinically and in patients and is considered a gold standard for visualization of viable hypoxic cells in biopsies. Furthermore, pimonidazole has shown promise as a marker of poor prognosis [5] and pimonidazole may therefore be useful to identify patients that benefit from hypoxic intervention. Surprisingly, thorough investigations of the usefulness of pimonidazole as a PET imaging agent have not been conducted. Specifically, pimonidazole, has a relatively short plasma half-life of approximately 30 minutes, which may ensure appropriate removal of unbound (hypoxia unrelated) compound before imaging. In this study we have labeled pimonidazole with ¹⁸F ([¹⁸F]PIMO), and tested its usefulness as a hypoxia marker in vitro and in tumor-bearing mice.

Material and methods

Radiochemistry

[¹⁸F]FPIMO was produced by the nucleophilic fluorination of 1-[2-*O*-tosyl-3-(2-nitroimidazole-1-yl)-propyl]-piperidine using the commercially available Fluorination Module (Scansystem). Firstly, [¹⁸F]Fluoride is produced by the ¹⁸O(p,n)¹⁸F nuclear reaction using a GE Medical Systems PETtrace 17 MeV cyclotron for bombardment of 2.6 ml ¹⁸O enriched water with high-energy protons. The [¹⁸F]fluoride was transferred, in a narrow bore teflon capillary, from the cyclotron to an automated fluorination synthesis module situated in a dedicated lead shielded area in the radiochemistry laboratory. The collected [¹⁸F]fluoride was trapped on a QMA cartridge and eluted off with kryptofix eluent into the reaction vial. Acetonitrile was added in three portions during 15 minutes, to facilitate drying and activation of [¹⁸F]fluoride. At the end of the drying process, the precursor solution (5–10 mg dissolved in 1 ml DMSO) was added and the reaction started for 5 minutes at 110°C. Before HPLC, the reaction solution was cooled to 20°C and diluted with 2 ml water. The HPLC system consisted of a Nucleosil C18 10 μm 250 × 10 mm column, and the eluent: 70 mM NaH₂PO₄ for 10 minutes, followed by 5% EtOH in 70 mM NaH₂PO₄ solution; flow: 5 ml/min; UV @ 254 nm and radiodetection. The fractions containing the two isomeric forms [¹⁸F]FPIMO “5” and [¹⁸F]FPIMO “6” eluted after approximately 16 minutes and 18 minutes, respectively. The desired fraction was collected, passed through a sterile filter and into a sterile vial. The final product contained about 0.25–1.0 GBq [¹⁸F]FPIMO “5” or “6” in 10 ml solution. Quality control showed both products to be >91% radiochemically pure. [¹⁸F]FAZA was produced as detailed in a previous study [4].

Cell studies

Human cervical (SiHa) and head and neck (FaDu_{DD}) squamous cell carcinoma cells were grown under conventional cell culturing conditions as recommended by the supplier. Prior to experiments, cells were seeded in 75 μl D-MEM medium layered on 9 mm circular glass coverslips positioned in compartmentalized Petri dishes. This set-up allows incubation of multiple cover slips and cell lines simultaneous, while cells are sharing a common pool of medium/tracer, which minimizes unintentionally experimental variation (for further details see [23]). Following cell adhesion (>6 hours), 20 ml of D-MEM was gently added to each Petri dish and cells were allowed to grow until confluent. For experiments, cells were transferred to custom-built airtight chambers placed

in a cell incubator, and incubated for one hour while being continuously flushed with humidified gas mixtures with 5% CO₂ and variable oxygen content (see [23]). Following this pre-equilibration period, [¹⁸F]FPIMO dissolved in ~0.3 ml degassed saline was added through small sealable holes (without compromising the chamber gas composition), and cells were allowed to incubate for an additional three hours. Finally, cells were washed three times with ~20 ml saline per wash. Each coverslip (four per cell line and per oxygen tension) containing attached cells were transferred to scintillation vials and radioactivity was determined using a Packard well counter. To assess whether hypoxia-induced and baseline tracer binding is irreversible, coverslips that previously had been subjected to three hours of normoxia or anoxia in the presence of tracer, were quickly washed in saline and transferred to a tracer free medium and incubated for another one hour under normoxic conditions. Subsequently, cells were washed and analyzed for radioactivity as described above and the results were compared to radioactivity measured prior to reincubation.

Animal studies

The murine mammary adenocarcinoma C3H and the murine squamous cell carcinoma SCCVII were established as subcutaneous tumors in CDF1 and C3H/HeNTac mice, respectively, as previously described [4,24]. Furthermore, the human tumor models SiHa and FaDu_{DD} were grown as subcutaneous tumors in immune-compromised NMRI nude mice [4]. Mice were used for experiments when tumors reached a size of 200–500 mm³ (foot tumors) and up to 1000 mm³ (flank/back) two to eight weeks after inoculation. Unanesthetized mice were immobilized in transparent PVC tubes and administered with [¹⁸F]FPIMO or [¹⁸F]FAZA in 0.2 to 0.4 ml saline in the tail vein, and intra-peritoneally with 60 mg/kg (0.02 ml/g) of unlabeled pimonidazole (for immunohistochemical detection of hypoxia) and returned to their cages. Some mice were anesthetized in 2% isoflurane and PET scanned for 5 minutes before sacrifice using a Concorde R4 microPET. PET images were reconstructed as described elsewhere [4]. Tumors and reference tissues (blood and muscle) and other organs of interest were excised at various time points. Tissue samples were weighed and analyzed for radioactivity using a Packard well counter and results were expressed as tumor-to-reference tissue ratios or standardized uptake values (SUVs). SUV was calculated as the activity concentration (CPM/g) in the tissue (corrected to time of injection) times the body weight divided by injected dose. Furthermore, for autoradiographic

and immune-histological analysis, tumor and muscle tissue were frozen in pre-cooled (–40°C) isopentane, and multiple consecutive 10 μm tissue cryosections were prepared. Dried tissue sections were placed in cassettes and overlaid with phosphor imaging plates and left overnight. Finally, the intra-tissue tracer signal distribution was extracted at a pixel size of 25 μm using a Fuji BAS 5000 scanner. Some of the tumor tissue sections previously analyzed using autoradiography, were immunologically stained for the distribution of pimonidazole (viable cells with pO₂ < 10 mmHg) using a previously described protocol [25]. Pimonidazole stained tissue sections were digitalized using a Hamamatsu NanoZoomer tissue section scanner and compared to the corresponding autoradiograms. All animal experiments were performed under the national and European Union approved guidelines for animal welfare.

Statistical analysis

Results are presented as mean values ± SEM. Statistical significances were evaluated by using the Student's t-test, with a significance level of p < 0.05.

Results

Due to spontaneous isomeric rearrangement, synthesis of [¹⁸F]FPIMO led to the formation of two products, which were named isomer “5” and “6”. The key reactions of the [¹⁸F]FPIMO synthesis and the molecular structure of the two originating isomers are presented in Figure 1. Since the usefulness of these isomers for PET hypoxia imaging may differ, both were tested separately. Firstly, we tested [¹⁸F]FPIMO in cell culture studies which revealed that

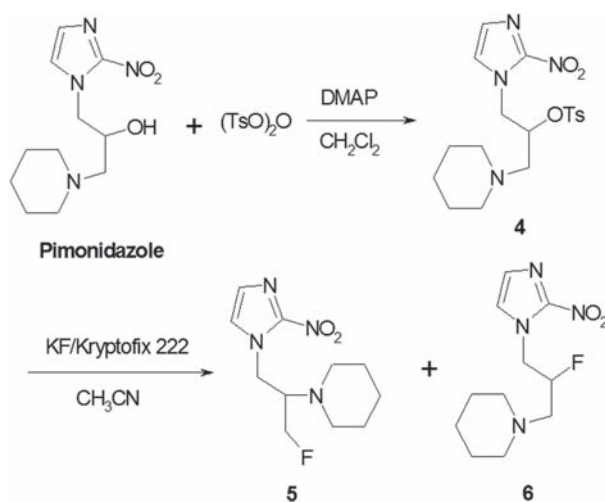


Figure 1. [¹⁸F]FPIMO synthesis overview showing the molecular structure of the tosylated precursor and the two resulting ¹⁸F-labeled, spontaneously convertible, isomers named “5” and “6”.

cellular uptake of [¹⁸F]FPIMO was hugely stimulated by anoxia, but retention differed profoundly between the two isomers. For isomer “6”, anoxic-to-normoxic tracer ratios following three hours of tracer incubation reached values of 13 ± 4 and 29 ± 9 for FaDu_{DD} and SiHa cells, respectively ($n = 2$). The corresponding ratios for isomer “5” were much higher, reaching values of 36 ± 4 and 102 ± 15 for FaDu_{DD} and SiHa, respectively ($n = 4$). The binding ratio for isomer “5” was significantly higher for SiHa than for FaDu_{DD} cells. Re-incubation of tracer-loaded cells in well-oxygenated tracer free medium for one hour (only performed for isomer “5”) resulted in some loss of tracer, suggesting that hypoxia-driven binding is not entirely irreversible. For cells previously tracer-loaded under anoxic conditions, tracer loss was $26 \pm 3\%$ and $21 \pm 6\%$ for FaDu_{DD} and SiHa cells, respectively ($n = 3$). The same numbers for cells previously incubated under oxidic conditions, were $44 \pm 6\%$ and $62 \pm 10\%$, for FaDu_{DD} and SiHa cells, respectively ($n = 3$).

Although in vitro tracer binding capacity was higher for SiHa than for FaDu_{DD} cells, FaDu_{DD} tumors retained more tracer (isomer “5”) than SiHa when quantified relative to non-hypoxic reference tissues, suggesting that FaDu_{DD} is a more hypoxic tumor. Tumor-to-muscle activity ratios reached 3.3 ± 0.5 and 6.1 ± 0.3 three hours after tracer administration for SiHa and FaDu_{DD}, respectively. Tumor-to-blood ratios were somewhat lower, and reached values of 2.3 ± 0.6 and 3.1 ± 0.2 in mice bearing SiHa and FaDu_{DD} tumors, respectively. $n = 4$ for SiHa and $n = 3$ for FaDu_{DD}. [¹⁸F]FPIMO isomer “5” was further tested in mice bearing murine SCCVII tumors, where tumor-to-reference tissue ratios also revealed retention in tumor tissue (Figure 2B), which was clearly related to tumor hypoxia (see matching autoradiogram and pimonidazole map for SCCVII in Figure 2). Isomer “6” was tested in mice bearing SCCVII tumors, which resulted in tumor-to-reference tissue ratios that were comparable to the results for isomer “5”, three hours post-injection (compare Figure 2B and D). Tumor-to-reference tissue ratios increased somewhat over time for isomer “6” (Figure 2D).

In two of our tumor models, we also performed a direct comparison of [¹⁸F]FPIMO (isomer “5”) with the well-established PET hypoxia tracer [¹⁸F]FAZA. In SCCVII tumors, tumor-to-blood and tumor-to-muscle ratios were comparable for the two tracers, whereas [¹⁸F]FAZA proved superior in the C3H tumor model (Figure 2). In both tumor models, intra-tumoral tracer contrast, as evaluated from autoradiograms, was better for [¹⁸F]FAZA which demonstrated less background in viable non-hypoxic areas (e.g. with the C3H tumor see Figure 2). Another

important difference between [¹⁸F]FPIMO and [¹⁸F]FAZA was the observation that the absolute levels of tumor tracer retention (reported as SUV values), was much higher for [¹⁸F]FAZA than for [¹⁸F]FPIMO (Figure 2C), which also was clearly evident from PET scans which revealed that tumors were not clearly visualized in animals administered with [¹⁸F]FPIMO (e.g. see Figure 3).

Biodistribution data (Figure 3) partly explains the reason for the low tumor SUVs, since they showed that a very high fractions of [¹⁸F]FPIMO (or its metabolites) accumulates in the liver and kidney, where it is probably metabolized or excreted, thus reducing tumor tracer availability. PET images (Figure 3) clearly highlighted this inappropriate tracer distribution, which resulted in very poor tumor visualization for [¹⁸F]FPIMO compared to [¹⁸F]FAZA. Furthermore, radio-HPLC analysis of blood samples collected from mice at various time points following tracer administration, revealed an extremely fast metabolism of [¹⁸F]FPIMO to unwanted metabolites, with very little parent compound remaining 15 minutes post-injection (not shown). Similar results were obtained in rats (not shown).

Discussion

Thorough evaluation of possible new PET hypoxia markers is a multistep process. Ideally it should involve testing in simple cell systems with accurate control of microenvironmental conditions (e.g. pO₂) to verify binding mechanisms. Furthermore, in vivo testing is crucial and, besides crude measures such as tumor-to-reference tissue ratios, it should be supplemented with high-resolution invasive analysis to verify that the tracer co-localizes with other established markers of hypoxia. Furthermore, a head-to-head comparison in the same tumor models with other PET tracers should ideally be performed, although this is often not the case.

In this study, all of the listed approaches were used. Initially, we showed that [¹⁸F]FPIMO performs excellently in vitro in two different cell lines, although a large difference between the two isomers was observed. The anoxic-to-oxic ratios observed for isomer “5” was similar to (for FaDu_{DD}) or better than (for SiHa) values previously reported for [¹⁸F]FAZA, using the same experimental setup [23]. The reason for the difference between the two isomers is unknown, but enzymatic recognition and bioreduction may differ hugely among closely related compounds. The reason for the large cell line difference is also unknown, but substantial cell-to-cell line variability has been reported for [¹⁸F]FMISO [26]. Since pimonidazole is a weak base, some of the difference may relate to differences in intra-cellular

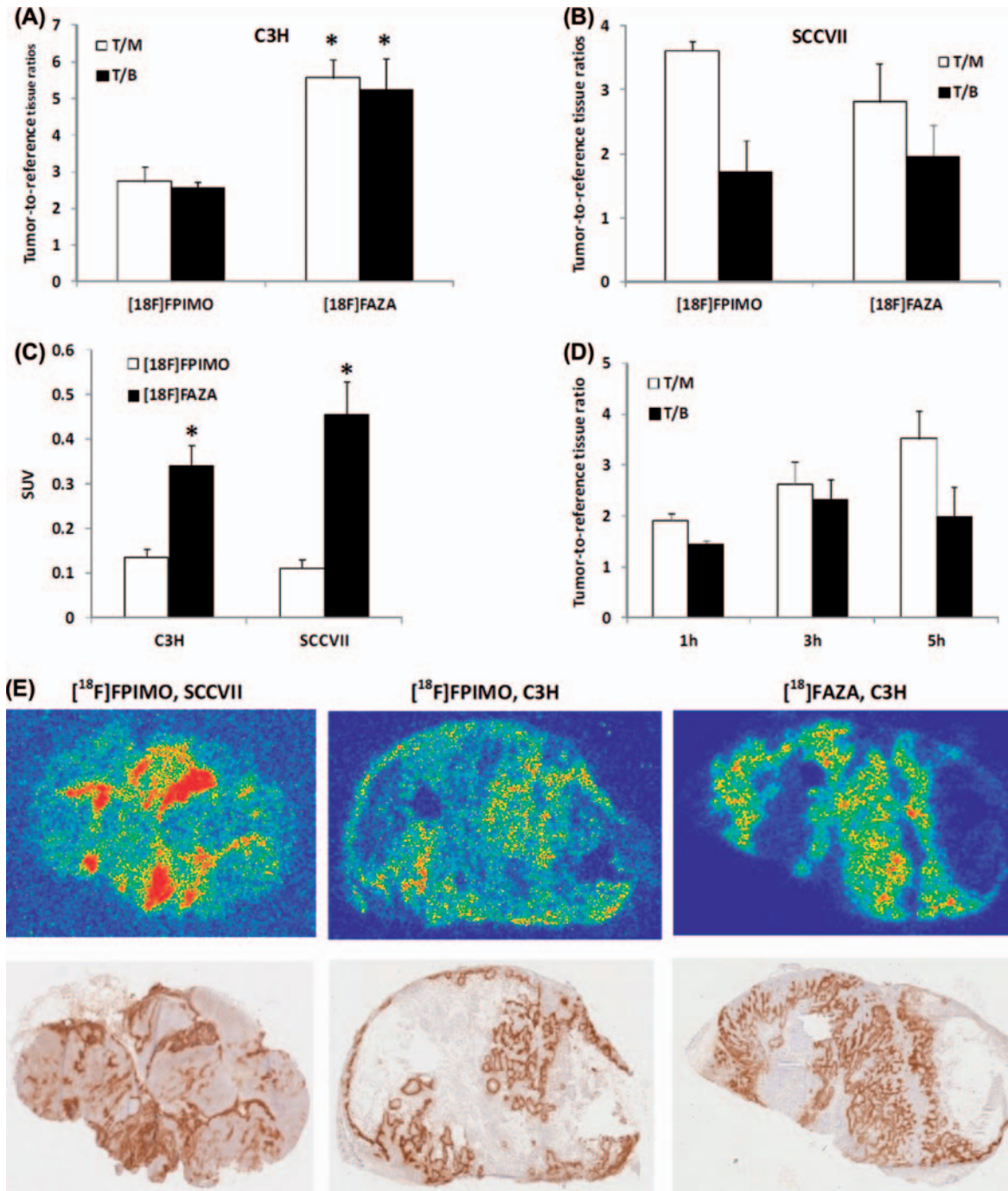


Figure 2. Head-to-head comparison of $[^{18}\text{F}]$ FPIMO (isomer “5”) and $[^{18}\text{F}]$ FAZA in two different murine tumor models (C3H and SCCVII) measured 3 hours following administration of tracer (A–C). For comparison, also tumor-to-reference tissue values obtained for isomer “6” in SCCVII tumors at various sampling time points, are included (D). In the C3H model (A), tumor-to-reference tissue ratios were significantly higher for $[^{18}\text{F}]$ FAZA than for $[^{18}\text{F}]$ FPIMO, whereas no significant difference was observed in the SCCVII tumor model (B). In both tumor models, SUV values were significantly lower for $[^{18}\text{F}]$ FPIMO than for $[^{18}\text{F}]$ FAZA (C). The corresponding autoradiograms and pimonidazole stainings show that both $[^{18}\text{F}]$ FPIMO and $[^{18}\text{F}]$ FAZA is retained in hypoxic tumor areas, but intra-tumoral contrast is somewhat better for $[^{18}\text{F}]$ FAZA in the C3H tumor (less $[^{18}\text{F}]$ FAZA signal in non-hypoxic viable tissue despite similar signal for the two tracers in hypoxic areas). Values are means \pm SEM, $n \geq 3$. *Denotes a significant difference between $[^{18}\text{F}]$ FPIMO and $[^{18}\text{F}]$ FAZA ($p < 0.05$).

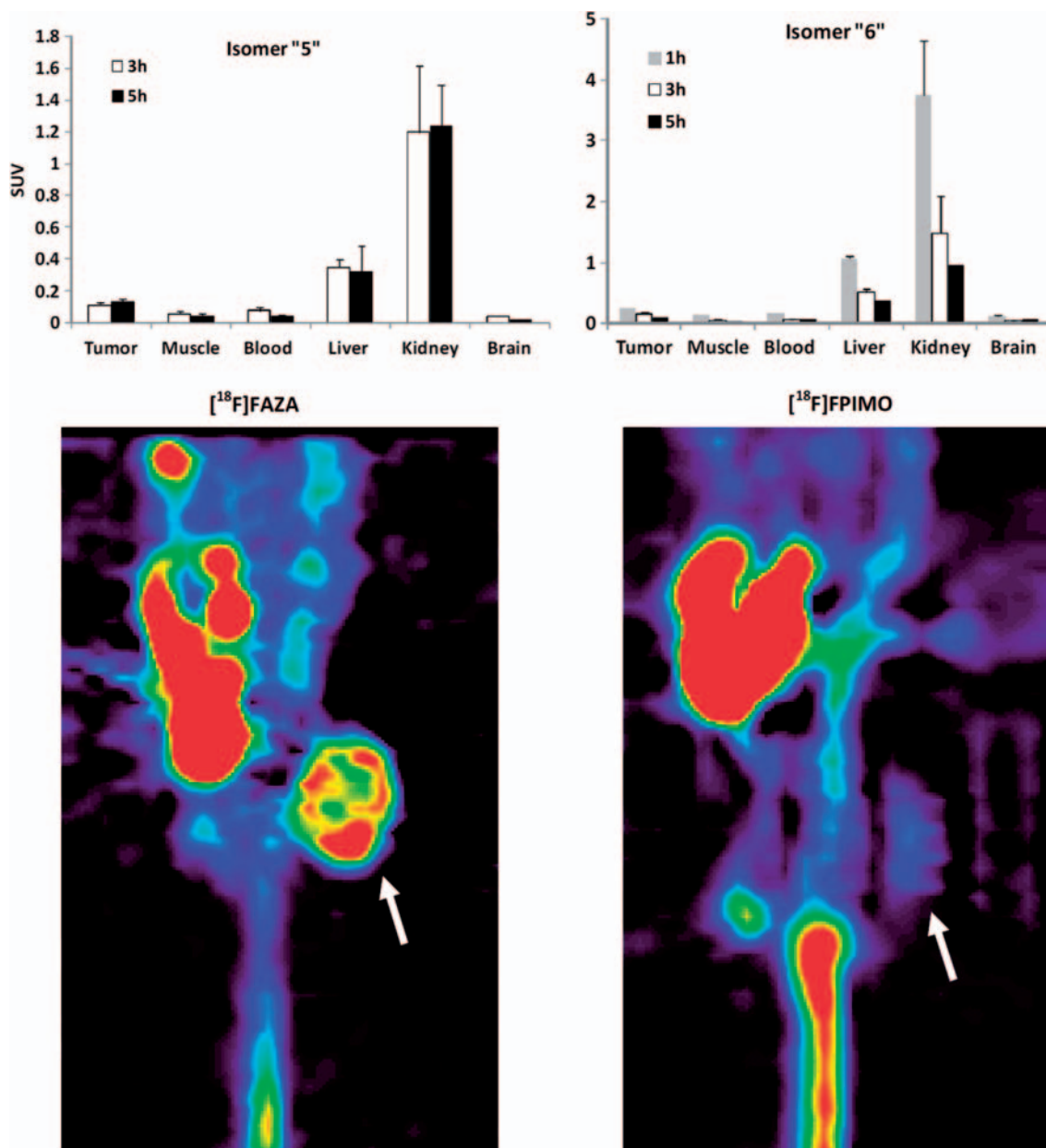


Figure 3. [^{18}F]FPIMO biodistribution data for tumor-bearing mice obtained at different post-injection times. Biodistribution of isomer "5" obtained in C3H/HeNHsd mice bearing SCCVII tumors. Upper left panel shows data for isomer "5" and upper right panel shows data for isomer "6". The sagittal-view PET images shows a direct comparison of [^{18}F]FAZA and [^{18}F]FPIMO in mice bearing tumors at their lower backs (white arrows shows the tumor position). Images were obtained 3 hours following tracer administration. Values are means \pm SEM. $n = 4$ for isomer "5" and $n = 5$ for isomer "6".

cytosolic or intra-lysosomal pH between cell lines which likely will affect the distribution of unbound pimonidazole [27].

Despite the encouraging in vitro results, [^{18}F]FPIMO performed rather poorly in vivo, when compared directly with the well-established PET tracer [^{18}F]FAZA. Although [^{18}F]FPIMO accumulated in tumors compared to typical reference tissues and strongly co-localized with the distribution of pimonidazole-adducts, the absolute levels of

[^{18}F]FPIMO in tumor tissue remained low for both isomers (Figure 2). A head-to-head comparison with [^{18}F]FAZA in the same batches of inoculated mice, revealed that SUV values were three to four-fold lower for [^{18}F]FPIMO. Higher SUV values have also been reported for [^{18}F]FMISO in tumor-bearing mice [28]. Knowing that low absolute tumor signal is a problem inherent to hypoxia imaging using nitroimidazole-based tracers, a further decrease by a factor of three to four is very

problematic, as clearly demonstrated in the PET images in Figure 3. The fundamental problem with labeled pimonidazole, seems to relate to its very fast metabolism as indirectly suggested by the biodistribution data, which shows very high radioactivity in organs associated with excretion and metabolism for both isomers (Figure 3). In PET hypoxia imaging, a delicate balance between the need for clearance of unbound tracer and a reasonable availability of tracer for binding (favorable input function) exists. Therefore, tracer removal from the blood by various non-target organs could in principle be advantageous. In the case of [^{18}F]FPIMO, however, removal of tracer from the blood may be too rapid to allow for appropriate tissue binding. Furthermore, direct measurements of metabolites using radio-HPLC, in blood samples drawn from mice or rats showed that [^{18}F]FPIMO is not simply removed from the circulation, but also metabolized to unwanted metabolites that are present in the circulation. Although, assessment of blood metabolites were only evaluated for isomer “6”, the biodistribution data strongly suggest that the two isomers share this problem (Figure 3). The biodistribution data for [^{18}F]FPIMO differs profoundly from similar data obtained in two different studies using [^{18}F]FAZA and [^{18}F]FMISO in tumor-bearing mice, where tumor activity was comparable to or higher than in liver and kidneys three hours after tracer administration [20,29]. Pimonidazole has previously been evaluated thoroughly as a possible radiosensitizer and there is no evidence to suggest that unlabeled pimonidazole is rapidly metabolized (within minutes) to other compounds, as plasma half-lives ranges from 30 minutes in mice to several hours in patients.

Preferably, future research should focus on labeling of pimonidazole in another position (e.g. at the four-position in the six-membered heterocyclic ring – Figure 1), although such labeling is complex. However, even the usefulness of the two isomers tested in the previous study cannot be decisively dismissed based on the current study, since metabolism may differ in non-rodent animals, and further testing of the two isomers in other mammalian species are justified.

Declaration of interest: The authors report no conflicts of interest. The authors alone are responsible for the content and writing of the paper. This work has been funded with the support of the METOXIA project no. 222741 under the 7th Research Framework Programme of the European Union and by CIRRO – The Lundbeck Foundation Center for Interventional Research in Radiation Oncology, and the Danish Cancer Society.

References

- [1] Vaupel P. Tumor microenvironmental physiology and its implications for radiation oncology. *Semin Radiat Oncol* 2004;14:198–206.
- [2] Brown JM. Tumor microenvironment and the response to anticancer therapy. *Cancer Biol Ther* 2002;1:453–8.
- [3] Overgaard J. Hypoxic radiosensitization: Adored and ignored. *J Clin Oncol* 2007;25:4066–74.
- [4] Busk M, Horsman MR, Jakobsen S, Keiding S, van der Kogel AJ, Bussink J, et al. Imaging hypoxia in xenografted and murine tumors with ^{18}F -fluoroazomycin arabinoside: A comparative study involving microPET, autoradiography, PO2-polarography, and fluorescence microscopy. *Int J Radiat Oncol Biol Phys* 2008;70:1202–12.
- [5] Kaanders JH, Wijffels KI, Marres HA, Ljungkvist AS, Pop LA, van den Hoogen FJ, et al. Pimonidazole binding and tumor vascularity predict for treatment outcome in head and neck cancer. *Cancer Res* 2002;62:7066–74.
- [6] Busk M, Toustrup K, Sorensen BS, Alsner J, Horsman MR, Jakobsen S, et al. In vivo identification and specificity assessment of mRNA markers of hypoxia in human and mouse tumors. *BMC Cancer* 2011;11:63.
- [7] Sorensen BS, Toustrup K, Horsman MR, Overgaard J, Alsner J. Identifying pH independent hypoxia induced genes in human squamous cell carcinomas in vitro. *Acta Oncol* 2010;49:895–905.
- [8] Toustrup K, Sorensen BS, Nordmark M, Busk M, Wiuf C, Alsner J, et al. Development of a hypoxia gene expression classifier with predictive impact for hypoxic modification of radiotherapy in head and neck cancer. *Cancer Res* 2011;71:5923–31.
- [9] Toustrup K, Sorensen BS, Lassen P, Wiuf C, Alsner J, Overgaard J. Gene expression classifier predicts for hypoxic modification of radiotherapy with nimorazole in squamous cell carcinomas of the head and neck. *Radiother Oncol* 2012;102:122–9.
- [10] Hendrickson K, Phillips M, Smith W, Peterson L, Krohn K, Rajendran J. Hypoxia imaging with [^{18}F] FMISO-PET in head and neck cancer: Potential for guiding intensity modulated radiation therapy in overcoming hypoxia-induced treatment resistance. *Radiother Oncol* 2011;101:369–75.
- [11] Toma-Dasu I, Uhrdin J, Antonovic L, Dasu A, Nuyts S, Dirix P, et al. Dose prescription and treatment planning based on FMISO-PET hypoxia. *Acta Oncol* 2012;51: 222–30.
- [12] Tran LB, Bol A, Labar D, Jordan B, Magat J, Mignon L, et al. Hypoxia imaging with the nitroimidazole ^{18}F -FAZA PET tracer: A comparison with OxyLite, EPR oximetry and ^{19}F -MRI relaxometry. *Radiother Oncol* 2012;105:29–35.
- [13] Zips D, Zophel K, Abolmaali N, Perrin R, Abramyuk A, Haase R, et al. Exploratory prospective trial of hypoxia-specific PET imaging during radiochemotherapy in patients with locally advanced head-and-neck cancer. *Radiother Oncol* 2012;105:21–8.
- [14] Horsman MR, Mortensen LS, Petersen JB, Busk M, Overgaard J. Imaging hypoxia to improve radiotherapy outcome. *Nat Rev Clin Oncol* 2012;9:674–87.
- [15] Mortensen LS, Johansen J, Kallehauge J, Primdahl H, Busk M, Lassen P, et al. FAZA PET/CT hypoxia imaging in patients with squamous cell carcinoma of the head and neck treated with radiotherapy: Results from the DAHANCA 24 trial. *Radiother Oncol* 2012;105:14–20.
- [16] Rasey JS, Koh WJ, Grierson JR, Grunbaum Z, Krohn KA. Radiolabelled fluoromisonidazole as an imaging agent for tumor hypoxia. *Int J Radiat Oncol Biol Phys* 1989;17: 985–91.

- [17] Abolmaali N, Haase R, Koch A, Zips D, Steinbach J, Baumann M, et al. Two or four hour [¹⁸F]FMISO-PET in HNSCC. When is the contrast best? *Nuklearmedizin* 2011;50:22–7.
- [18] Busk M, Horsman MR, Overgaard J. Resolution in PET hypoxia imaging: Voxel size matters. *Acta Oncol* 2008;47:1201–10.
- [19] Chen L, Zhang Z, Kolb HC, Walsh JC, Zhang J, Guan Y. ¹⁸F-HX4 hypoxia imaging with PET/CT in head and neck cancer: A comparison with ¹⁸F-FMISO. *Nucl Med Commun* 2012;33:1096–102.
- [20] Piert M, Machulla HJ, Picchio M, Reischl G, Ziegler S, Kumar P, et al. Hypoxia-specific tumor imaging with ¹⁸F-fluoroazomycin arabinoside. *J Nucl Med* 2005;46:106–13.
- [21] Souvatzoglou M, Grosu AL, Roper B, Krause BJ, Beck R, Reischl G, et al. Tumour hypoxia imaging with [¹⁸F]FAZA PET in head and neck cancer patients: A pilot study. *Eur J Nucl Med Mol Imaging* 2007;34:1566–75.
- [22] Kleiter MM, Thrall DE, Malarkey DE, Ji X, Lee DY, Chou SC, et al. A comparison of oral and intravenous pimonidazole in canine tumors using intravenous CCI-103F as a control hypoxia marker. *Int J Radiat Oncol Biol Phys* 2006;64:592–602.
- [23] Busk M, Horsman MR, Jakobsen S, Bussink J, van der Kogel A, Overgaard J. Cellular uptake of PET tracers of glucose metabolism and hypoxia and their linkage. *Eur J Nucl Med Mol Imaging* 2008;35:2294–303.
- [24] Mortensen LS, Busk M, Nordmark M, Jakobsen S, Theil J, Overgaard J, et al. Assessing radiation response using hypoxia PET imaging and oxygen sensitive electrodes: A preclinical study. *Radiother Oncol* 2011;99:418–23.
- [25] Busk M, Munk OL, Jakobsen S, Wang T, Skals M, Steiniche T, et al. Assessing hypoxia in animal tumor models based on pharmacokinetic analysis of dynamic FAZA PET. *Acta Oncol* 2010;49:922–33.
- [26] Rasey JS, Nelson NJ, Chin L, Evans ML, Grunbaum Z. Characteristics of the binding of labeled fluoromisonidazole in cells in vitro. *Radiat Res* 1990;122:301–8.
- [27] Dennis MF, Stratford MR, Wardman P, Watts ME. Cellular uptake of misonidazole and analogues with acidic or basic functions. *Int J Radiat Biol Relat Stud Phys Chem Med* 1985;47:629–43.
- [28] Oehler C, O'Donoghue JA, Russell J, Zanzonico P, Lorenzen S, Ling CC, et al. ¹⁸F-fluoromisonidazole PET imaging as a biomarker for the response to 5,6-dimethylxanthenone-4-acetic acid in colorectal xenograft tumors. *J Nucl Med* 2011;52:437–44.
- [29] Reischl G, Dorow DS, Cullinane C, Katsifis A, Roselt P, Binns D, et al. Imaging of tumor hypoxia with [¹²⁴I]IAZA in comparison with [¹⁸F]FMISO and [¹⁸F]FAZA – first small animal PET results. *J Pharm Pharm Sci* 2007;10:203–11.